Galaxy Evolution and Feedback across Different Environments
Proceedings IAU Symposium No. 359, 2020
T. Storchi-Bergmann, W. Forman, R. Overzier & R. Riffel, eds.
doi:10.1017/S1743921320004226

Cold gas studies of a z = 2.5 protocluster

Minju M. Lee[1], Ichi Tanaka[2] and Rohei Kawabe[3,4,5]

[1]Max-Planck-Institut für Extraterrestrische Physik (MPE), Giessenbachstr. 1, D-85748 Garching, Germany

[2]Subaru Telescope, National Astronomical Observatory of Japan, 650 North Aohoku Place, Hilo, HI 96720, USA

[3]National Astronomical Observatory of Japan, 2-21-1 Osawa, Mitaka, Tokyo 181-8588, Japan

[4]The Graduate University for Advanced Studies (SOKENDAI), 2-21-1 Osawa, Mitaka, Tokyo 181-8588, Japan

[5]Department of Astronomy, The University of Tokyo, 7-3-1 Hongo, Bunkyo, Tokyo 113-0033, Japan

Abstract. We present studies of a protocluster at $z = 2.5$, an overdense region found close to a radio galaxy, 4C 23.56, using ALMA. We observed 1.1 mm continuum, two CO lines (CO (4–3) and CO (3–2)) and the lower atomic carbon line transition ([C I](^{3}P$_1$-^{3}P$_0$)) at a few kpc (0″.3-0″.9) resolution. The primary targets are 25 star-forming galaxies selected as Hα emitters (HAEs) that are identified with a narrow band filter. These are massive galaxies with stellar masses of $>10^{10}\,M_\odot$ that are mostly on the galaxy main sequence at $z = 2.5$. We measure the molecular gas mass from the independent gas tracers of 1.1 mm, CO (3–2) and [C I], and investigate the gas kinematics of galaxies from CO (4–3). Molecular gas masses from the different measurements are consistent with each other for detection, with a gas fraction ($f_{\rm gas} = M_{\rm gas}/(M_{\rm gas} + M_{\rm star})$) of $\simeq$0.5 on average but with a caveat. On the other hand, the CO line widths of the protocluster galaxies are typically broader by $\sim$50% compared to field galaxies, which can be attributed to more frequent, unresolved gas-rich mergers and/or smaller sizes than field galaxies, supported by our high-resolution images and a kinematic model fit of one of the galaxies. We discuss the expected scenario of galaxy evolution in protoclusters at high redshift but future large surveys are needed to get a more general view.

Keywords. galaxies: clusters: general, galaxies: evolution, galaxies: high-redshift, galaxies: ISM, galaxies: kinematics and dynamics, large-scale structure of universe

1. Introduction

Over the past two decades, multi-wavelength studies have provided a detailed picture of 'baryonic cycle'. Dust and CO observations revealed that the global (i.e., a few kpc scale) gas content, which fuels the star-forming activity, increases toward higher-z. The cosmic star-formation rate density peaked at $z \approx 1.5-2.5$, and has declined since then by a factor of 10-15 (e.g., Madau & Dickinson 2014). Together with a moderate or little evolution of star-forming efficiency, the observed gas content explains the observed cosmic star-formation rate density (e.g., Scoville *et al.* 2013; Genzel *et al.* 2015; Tacconi *et al.* 2018). A simple bath tub model (e.g., Bouché *et al.* 2010) or gas regulator model (e.g., Lilly *et al.* 2013) works remarkably well to describe such trends. However, such measurements are obtained for field galaxies and observations of members of dense, massive clusters and their progenitors are needed for a complete picture of 'baryonic cycle' across the Universe.

The kinematical properties are additional parameters that one needs to take into account to fully understand galaxy evolution. Typically, massive quiescent galaxies are short of star-forming activities with higher bulge-to-total mass ratio, meaning that star-forming galaxies need to not only stop their star formation activities but also change their appearance to become quiescent galaxies. The morphology-density relation has been known for four decades which shows an observational trend that the fraction of early-type galaxies, which are massive quiescent galaxies, increases in denser environment of clusters (Dressler 1980). However, it is still an open question whether environment is an additional parameter regulating the galaxy evolution which is more elusive for higher redshift. To aim for answering the question, we investigate both the gas content and gas kinematics using ALMA targeting a protocluster at $z = 2.5$ as a pilot study to fully understand galaxy evolution.

2. 4C 23.56 protocluster and parent sample

Protocluster 4C 23.56 was identified as an overdense region of the narrow-band(NB) selected Hα emitters in the vicinity of radio galaxy, 4C 23.56. It was targeted as a part of the MAHALO-Subaru (MApping HAlpha and Lines of Oxygen with Subaru) survey (Kodama *et al.* 2015).

There are rich ancillary data sets from X-ray to radio, which makes the protocluster an ideal target for a pilot study. Currently, the protocluster is known to have (projected) overdensities of differently selected galaxy populations, for example, mass-selected distant red galaxies (DRGs) (Kajisawa *et al.* 2006), extremely red objects (EROs; Knopp & Chambers 1997), IRAC (Mayo *et al.* 2012), MIPS (Galametz *et al.* 2012) sources, and SMGs observed at 1.1 mm (K. Suzuki 2013 PhD thesis; Zeballos *et al.* 2018).

We focus on HAEs as a primary target because they have relatively secure redshift information compared to other galaxy populations. We use the broadband emissions in J and Ks bands and NB Hα emissions to derive stellar masses and star-formation rate (SFR), respectively. The massive ($>10^{10}\,M_{\odot}$) galaxies are on the galaxy main sequence (MS) at $z = 2.5$ except for two. One of these two galaxies is the radio galaxy whose SFR may be overestimated by the AGN contamination. More details are described in Lee *et al.* (2017).

3. Gas content

We observed 1.1 mm dust continuum, CO (3–2) and [C I](^{3}P$_1$-^{3}P$_0$) (hereafter, [C I] (1–0)) using ALMA to measure the global gas content of the galaxies. Seven HAEs are detected in CO (3–2) line, four out of which are also detected in 1.1 mm continuum. Provided that the HAEs are mostly on the main-sequence, the typical gas recipes of dust (Scoville *et al.* 2013) and CO (Genzel *et al.* 2015) are applied to measure the gas content. We confirm that the methods are still valid for the members of the protocluster, and two different tracers provide consistent values within a factor 3 (Lee *et al.* 2017).

These measurements are revisited using [C I] (1–0) line, which is another independent gas tracer (Lee *et al.* 2021 in preparation). We detected the line in three galaxies. These include galaxies previously detected in CO (3–2) and two out of them also have dust continuum detection that allow us to self-consistently weigh the gas content from three different tracers. Figure 1 shows how the CO (3–2) luminosities are scaled with the [C I] luminosities that are both proxies for gas mass. For [C I] detections, they are aligned with field galaxies. Assuming a nominal abundance ratio that is applied to milky-way like galaxies (i.e., $\log([\mathrm{C\,I}]/[\mathrm{H_2}]) = -4.8$, see e.g., Valentino *et al.* 2018), we measure the molecular gas masses that are consistent within a factor of 3 compared to the previous

https://doi.org/10.1017/S1743921320004226 Published online by Cambridge University Press

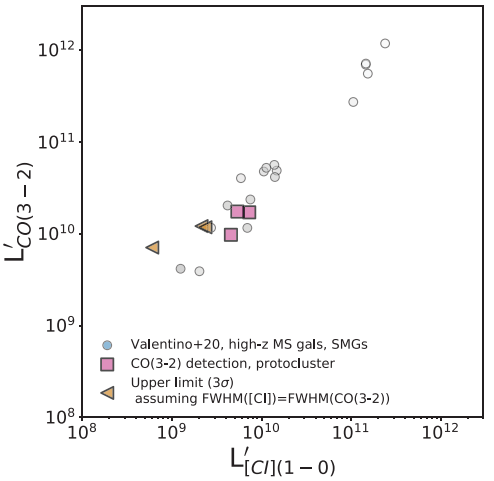

Figure 1. CO (3–2) line luminosity versus [C I] (1–0) line luminosity. Square symbol is for the [C I] (1–0) detection. The upper limit of [C I] (1–0) luminosity is obtained assuming the line width (FWHM) is the same as CO (3–2). For comparison, we also plot literature values compiled in Valentino *et al.* (2020) (Lee *et al.* 2020, in preparation).

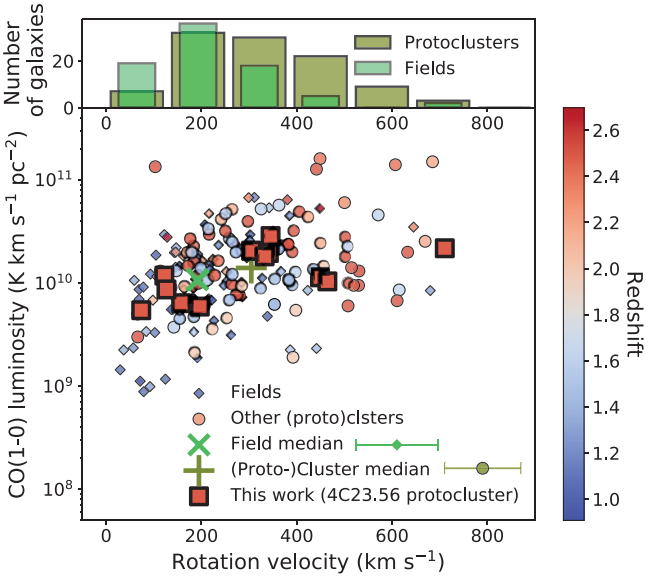

Figure 2. The distribution of the CO (1–0) luminosity and rotation velocity in the comparison with field galaxies. The rotation velocity is converted from the FWHM by taking the isotropic virial estimate of the circular velocity (FWHM$\times\sqrt{3/8\ln 2}$) to match with galaxies in Tacconi *et al.* (2013). The CO (1–0) luminosities are converted by assuming the line luminosity ratio of $R1J = 1.2$, 1.8, and 2.4 for $J = 2$, 3, and 4, respectively. Adapted from Lee *et al.* (2019).

measurements. We note that these are relatively gas-rich galaxies and less massive compared to the other [C I] non-detection galaxies. For [C I] non-detection, however, we find larger discrepancies, suggestive of different gas conditions or excitation toward more massive, gas-poorer systems, which needs deeper, other CO/[C I] observations to confirm. The details of the [C I] results are presented in Lee *et al.* (2020, in preparation). Overall, the

https://doi.org/10.1017/S1743921320004226 Published online by Cambridge University Press

(cold) gas fraction of the protocluster galaxies is $f_{\rm gas} = 0.5$ on average for the simultaneous detections (Lee *et al.* 2017) but there is a signature of different gas conditions for more massive, gas-poorer galaxies.

4. Gas kinematics

To probe the gas kinematics, we observed the protocluster galaxies with CO (4–3) at higher angular resolution of $0''.4$. Eleven HAEs are detected in CO (4–3), including six HAEs that were previously detected in CO (3–2) at a coarser angular resolution. The detections in both CO lines are broadly consistent in the line widths and the redshifts, confirming both detections. The CO (4–3) line detections confirm the redshifts of 11 HAEs, giving a constraint on the protocluster halo mass, which is a few $\times 10^{13}\,M_{\odot}$, supporting that the protocluster is a progenitor of Virgo-like clusters (Lee *et al.* 2019).

The CO line widths are on average broader by ≈50% compared to field galaxies, while the median CO luminosities are similar (Figure 2). Based on the resolved source structures and spectral analysis, we conclude that the broader line widths can be ascribed to unresolved gas-rich mergers and/or compact gas distribution. The compact gas distribution may be the result of gas-rich mergers but also of gas-stripping, which is difficult to confirm with the current available data sets and needs deeper observations to verify. Meanwhile, the best-fit kinematic parameters of one of the galaxies indicate that the specific angular momentum is similar to that of field populations during the cluster assembly and in the existence of gas-rich mergers, and hence "dissipational" processes are needed if it is a progenitor of early-type galaxies that are abundant in clusters (Lee *et al.* 2019).

5. Conclusions

We studied gas properties of galaxies using dust, CO and [C I] as a pilot project of studying protocluster galaxies. While the number of galaxies are limited, the cold gas studies provided rich information on the cold gas content and kinematical properties in detail. The different gas tracers of dust/CO/[C I] give consistent values of gas content with each other when [C I] line is detected. For protocluster 4C 23.56 at $z = 2.5$, the measured gas fraction is $f_{\rm gas} = 0.5$ on average comparable to field main-sequence galaxies at similar stellar mass range, but there is a hint of deviation when the stellar mass becomes larger ($\gtrsim 10^{11}\,M_{\odot}$), supported by the non-detection of [C I] and a tentative trend of a stronger stellar mass dependency of the gas depletion time scale. This also indicates the change of gas properties accordingly that one needs to confirm with other CO/[C I] transitions. We note that cold gas studies on different (proto)clusters at slightly lower redshift ($z = 1-2$) argued different gas fraction (larger/smaller than fields) that might be related to different evolutionary stages of cluster assembly (e.g., Noble *et al.* 2017; Coogan *et al.* 2018). Such differences may be an indicative of the change of the relative role of environment in different cluster phases at early times. For 4C 23.56, galaxies experience gas-rich mergers and some have compact sizes than field populations that may lead to fast consumption of gas and morpho-kinematic transformation, if most of the galaxies are progenitors of local early-type galaxies in clusters. Systematic surveys with a larger number of galaxies are needed to test the general picture of galaxy evolution in overdense regions.

References

Bouché, N., Dekel, A., Genzel, R., *et al.* 2010, *ApJ*, 718, 1001
Coogan, R. T., Daddi, E., Sargent, M. T., *et al.* 2018, *MNRAS*, 479, 703
Dressler, A. 1980, *ApJ*, 236, 351
Galametz, A., Stern, D., De Breuck, C., *et al.* 2012, *ApJ*, 749, 169
Genzel, R., Tacconi, L. J., Lutz, D., *et al.* 2015, *ApJ*, 800, 20
Kajisawa, M., Kodama, T., Tanaka, I., Yamada, T., & Bower, R. 2006, *MNRAS*, 371, 577

https://doi.org/10.1017/S1743921320004226 Published online by Cambridge University Press

Knopp, G. P. & Chambers, K. C. 1997, *ApJS*, 109, 367
Kodama, T., Hayashi, M., Koyama, Y., *et al.* 2015, in IAU Symposium, Vol. 309, Galaxies in 3D across the Universe, ed. B. L. Ziegler, F. Combes, H. Dannerbauer, & M. Verdugo, 255–258
Lee, M. M., Tanaka, I., Kawabe, R., *et al.* 2017, *ApJ*, 842, 55
—. 2019, *ApJ*, 883, 92
Lee, M. M., Tanaka, I., Iono, D., *et al.* 2021, e-prints, arXiv:2101.04691
Lilly, S. J., Carollo, C. M., Pipino, A., Renzini, A., & Peng, Y. 2013, *ApJ*, 772, 119
Madau, P. & Dickinson, M. 2014, *ARA&A*, 52, 415
Mayo, J. H., Vernet, J., De Breuck, C., *et al.* 2012, *A&A*, 539, A33
Noble, A. G., McDonald, M., Muzzin, A., *et al.* 2017, *ApJL*, 842, L21
Scoville, N., Arnouts, S., Aussel, H., *et al.* 2013, *ApJS*, 206, 3
Tacconi, L. J., Neri, R., Genzel, R., *et al.* 2013, *ApJ*, 768, 74
Tacconi, L. J., Genzel, R., Saintonge, A., *et al.* 2018, *ApJ*, 853, 179
Valentino, F., Magdis, G. E., Daddi, E., *et al.* 2018, *ApJ*, 869, 27
—. 2020, *ApJ*, 890, 24
Zeballos, M., Aretxaga, I., Hughes, D. H., *et al.* 2018, *MNRAS*, 479, 4577

https://doi.org/10.1017/S1743921320004226 Published online by Cambridge University Press